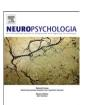


Contents lists available at SciVerse ScienceDirect

Neuropsychologia

journal homepage: www.elsevier.com/locate/neuropsychologia



Distinct subdivisions of the cingulum bundle revealed by diffusion MRI fibre tracking: Implications for neuropsychological investigations

D.K. Jones a,b, K.F. Christiansen R.J. Chapman J.P. Aggleton A,b,*

- ^a CUBRIC, School of Psychology, Cardiff University, Cardiff, CF10 3AT, United Kingdom
- ^b Cardiff Neuroscience and Mental Health Research Institute, Cardiff University, Cardiff, CF10 3AT, United Kingdom

ARTICLE INFO

Article history:
Received 24 June 2012
Received in revised form
25 October 2012
Accepted 13 November 2012
Available online 23 November 2012

Keywords: Cingulate cortex Hippocampus Prefrontal cortex Retrosplenial cortex White matter

ABSTRACT

The cingulum is a prominent white matter tract that supports prefrontal, parietal, and temporal lobe interactions. Despite being composed of both short and long association fibres, many MRI-based reconstructions (tractography) of the cingulum depict an essentially uniform tract that almost encircles the corpus callosum. The present study tested the validity of dividing this tract into subdivisions corresponding to the 'parahippocampal', 'retrosplenial', and 'subgenual' portions of the cingulum. These three cingulum subdivisions occupied different medial-lateral locations, producing a topographic arrangement of cingulum fibres. Other comparisons based on these different reconstructions indicate that only a small proportion of the total white matter in the cingulum traverses the length of the tract. In addition, both the radial diffusivity and fractional anisotropy of the subgenual subdivision differed from that of the retrosplenial subdivision which, in turn, differed from that of the parahippocampal subdivision. The extent to which the radial diffusivity scores and the fractional anisotropy scores correlated between the various cingulum subdivisions proved variable, illustrating how one subdivision may not act as a proxy for other cingulum subdivisions. Attempts to relate the status of the cingulum, as measured by MRI-based fibre tracking, with cognitive or affective measures will, therefore, depend greatly on how and where the cingulum is reconstructed. The present study provides a new framework for subdividing the cingulum, based both on its known connectivity and MRI-based properties.

© 2012 Elsevier Ltd. All rights reserved.

1. Introduction

The cingulum bundle is a prominent white matter tract that extends longitudinally above the corpus callosum. At its rostral limit the cingulum curves around the front of the genu of the corpus callosum while caudally it curves behind the splenium. Studies into the functional importance of the fibres in this bundle have been aided considerably in recent years by the relative ease with which the cingulum is revealed by diffusion MRI-based fibre tracking, i.e., tractography (Catani, Howard, Pajevic, & Jones, 2002; Jones, 2008). Such studies have examined the status of the cingulum bundle in conditions such as depression, traumatic brain injury, Mild Cognitive Impairment, Alzheimer's disease, and schizophrenia (e.g., Cullen et al., 2012; Jones et al., 2005a, 2006; Keedwell, Chapman, Christiansen, & Jones, 2012; Kubicki et al., 2003; Wu et al., 2010; Zhang et al., 2007).

Descriptions of the cingulum bundle have a long history, and it has been appreciated for over a century that the bundle contains many short association fibres, as well as longer fibres that potentially link the frontal lobe with the temporal lobes (Beevor, 1891;

Brodal, 1981; Schmahmann & Pandya, 2006). Detailed information about the composition of the primate cingulum bundle arrived with the introduction of axonal tracer studies in monkeys (Baleydier & Mauguiere, 1980; Goldman-Rakic, Selemon, & Schwartz, 1984; Morris, Petrides, & Pandya, 1999a; Morris, Pandya, & Petrides, 1999b; Mufson & Pandya, 1984; Vogt & Pandya, 1987; Vogt, Pandya, & Rosene, 1987). Such studies confirmed that the cingulum contains many afferent and efferent fibres associated with the rostral, mid, and caudal cingulate cortices (e.g., areas 23, 24, 25, 29, 30, 31, 32). These fibres include connections with sites such as the anterior thalamic nuclei, lateral dorsal thalamic nucleus, dorsolateral prefrontal cortex, and insula (Domesick, 1970; Goldman-Rakic et al., 1984; Mufson & Pandya, 1984; Petrides & Pandya, 2006; Vogt & Pandya, 1987). Other cingulum fibres are connected to structures in the temporal lobe, including the parahippocampal cortices, subicular cortices, and amygdala (Goldman-Rakic et al., 1984; Morris et al., 1999b; Mufson & Pandya, 1984). As a consequence, the cingulum bundle forms a complex tract comprised of many different connections with trajectories of different lengths (Schmahmann & Pandya, 2006). Due to its many short fibres, it is likely that different parts of the cingulum are principally composed of distinct white matter populations that are likely to reflect different underlying functions.

^{*} Corresponding author. Tel.: +2920 874563; fax: +2920 874858. E-mail address: aggleton@cardiff.ac.uk (J.P. Aggleton).

The complex composition of the cingulum is, however, rarely reflected in published diffusion MRI-based tractography images of the tract. These images often show a continuous band of white matter that seemingly links, uninterrupted, the medial temporal lobe with retrosplenial, anterior cingulate, prefrontal, and subgenual areas (e.g., Catani et al., 2002; Concha, Gross, & Beaulieu, 2005; Gong et al., 2005; Singh & Wong, 2010; Thiebaut de Schotten, Dell'Acqua, Valabregue, & Catani, 2012; Xie et al., 2005). Such images suggest an apparent continuity of fibres in the cingulum bundle, while anatomical tracing studies in nonhuman primates reveal the presence of numerous short association fibres (e.g., Mufson & Pandya, 1984).

This discrepancy may arise as an artifact of the way that tractography data are compiled. A common approach is to reconstruct multiple virtual fibre pathways (perhaps from every voxel in the dataset), and then to use anatomical regions of interest (ROIs) as 'waypoints' to 'virtually dissect' out the tract of interest (Conturo et al., 1999; Catani et al., 2002). Such ROIs can be used inclusively (e.g., the tract has to pass through multiple regions of interest to be retained for analysis) or exclusively (e.g., if the tract passes through this region, then it should be rejected). In keeping with Boolean logic, the inclusive ROIs are named 'AND' gates, and the exclusive ROIs as 'NOT' gates.

The most common practice of visualizing the cingulum bundle with tractography is to put single or multiple regions of interest dorsal to the body of the corpus callosum and to identify and retain those pathways that pass through the ROIs (Catani et al., 2002; Concha et al., 2005; Gong et al., 2005; Singh & Wong, 2010; Thiebaut de Schotten et al., 2012; Xie et al., 2005). A concern is that the cingulum bundle may actually comprise several, largely distinct subdivisions that only appear united due to the numerous short association fibres within this tract and the resulting overlap in their trajectories. The present study selected three potential subdivisions within the extent of the cingulum bundle ('parahippocampal', 'retrosplenial', and 'subgenual'). One of these subdivisions, the parahippocampal subdivision, was visualized in two different ways. One parahippocampal reconstruction ('unrestricted') used very similar logic to that applied to the other two potential cingulum subdivisions (subgenual and retrosplenial), and was intended to reveal the full extent of the tract. The second parahippocampal reconstruction ('restricted') was intended to segregate any parietal and occipital fibres, and so a 'NOT' gate was used to remove more rostral connections, e.g., those with the frontal lobe. For this reason, the second reconstruction is designated as the 'restricted' parahippocampal subdivision. The goal was to subdivide the cingulum even further to help isolate potential subdivisions at a finer level.

The questions addressed by this study included whether MRI-based tractography could help determine if these three cingulum subdivisions are likely to contain different fibre populations, and whether there are topographical differences within the tract. A further goal was to compare other characteristics, e.g., fractional anisotropy or radial diffusivity, across these same subdivisions. One purpose was to determine whether neuropsychological investigations that relate cingulum bundle status with cognition should focus on specific tract subdivisions or whether it is acceptable to generalize along the extent of the tract.

2. Materials and methods

2.1. Participant recruitment

Twenty right-handed women (mean age at scan=36.3 years, range 27–42) were recruited from the Cardiff Community panel, a cohort of volunteers drawn from the wider community that had agreed to be contacted about studies in the University. To avoid ongoing maturation effects, we limited our age range to >25

years, and to avoid documented ageing effects on diffusion MRI metrics, set an upper limit of 45 years. Finally, to reduce possible sources of variance, we opted to recruit a single gender. In this case, 20 right-handed females that satisfied the criteria were available from the panel. All participated under informed consent and the study was approved by the Ethics Committee of the School of Psychology in Cardiff University. Usual contraindications for MRI were applied (e.g., metallic implants, pacemakers, claustrophobia), and all participants were free from known neurological or psychiatric conditions.

2.2. Diffusion MRI scanning

Diffusion weighted MR data were acquired on a 3 T GE HD_x MRI system (General Electric Healthcare) with a peripherally-gated twice-refocused spin-echo echo-planar imaging sequence providing whole oblique axial (parallel to the commissural plane) brain coverage. Data were acquired from 60 slices of 2.4 mm thickness, with a field of view of 23 cm, and an acquisition matrix of 96×96 (yielding isotropic voxels of $2.4 \times 2.4 \times 2.4$ mm, reconstructed to a resolution of $1.9 \times 1.9 \times 2.4$ mm). TE (echo delay time) was 87 ms and parallel imaging (ASSET factor=2) was employed. Diffusion encoding gradients (b=1200 s/mm²) were applied along 60 isotropically-distributed directions (Jones, Horsfield, & Simmon, 1999) and six additional non-diffusion weighted scans were collected. The acquisition time was approximately 26 min.

2.3. Diffusion MRI data pre-processing

The data were corrected for distortions and subject motion using an affine registration to the non-diffusion-weighted images, with appropriate re-orienting of the encoding vectors (Leemans & Jones, 2009). A single diffusion tensor model was fitted (Basser, Mattiello, & LeBihan, 1994) to the data to allow quantitative parameters such as fractional anisotropy (FA) and radial diffusivity to be computed. Maps of FA were constructed for each participant. Constrained spherical harmonic deconvolution (CSD) was used to estimate the fibre orientation density function (fODF) in each voxel (Tournier, Calamante, Gadian, & Connelly, 2004).

2.4. Tract reconstructions

Deterministic tractography was carried out using *ExploreDTI* (Leemans, Jeurissen, Siibers, & Jones, 2009) following peaks in the fODF reconstructed from CSD (Jeurissen, Leemans, Jones, Tournier, & Sijbers, 2011). For each voxel in the data set, streamlines were initiated along any peak in the fODF that exceeded an amplitude of 0.1 (thus, multiple fibre pathways could be generated from any voxel). Each streamline continued, in 0.5 mm steps, following the peak in the ODF that subtended the smallest angle to the incoming trajectory. The termination criteria included: a turning angle of greater than 60° and an fODF amplitude threshold of 0.1. Once the 'whole brain tractography' was complete, regions of interest were drawn on the map of fractional anisotropy of each participant and subsequently used to dissect the cingulum bundle according to five closely-related protocols (Fig. 1).

All tract reconstructions were performed independently by two experimenters (KC, RC). For each reconstruction, the mean fractional anisotropy (FA) and mean radial diffusivity (RD) were obtained by averaging the FA and RD values sampled at 0.5 mm steps along the entire length of the tract (Jones, Travis, Eden, Pierpaoli, & Basser, 2005b). Prior to any systematic data collection, the two experimenters ran an initial set of pilot reconstructions using variable temporal lobe 'AND' gates. For the final reconstructions, specification of the locations for the AND and NOT gates was fixed against particular landmarks, so aiding the reproducibility of tract reconstruction.

For all of the various subdivision reconstructions the corpus callosum was first identified on the midsagittal slice. The next step was to find the parasagittal level in each hemisphere that provided the most extensive visualisation of the cingulum bundle. The position of the corpus callosum in that same plane was then used to derive a set of fixed landmarks for subsequent ROIs. The first reconstruction ('standard cingulum') adopted the inclusive strategy used in many studies whereby much of the full extent of the cingulum is visualized.

2.4.1. 'Standard cingulum' reconstruction (Fig. 1i)

The rostral–caudal midpoint of the body of the corpus callosum was first identified (Fig. 1i). This point was defined as the mid-way point between the back of the curve of the genu (i.e., its most posterior part at the flexure) and the front of the splenium (i.e., its most anterior part at the flexure). These callosal sites are indicated by the arrows in Fig. 1i. From this midpoint, the coronal sections that were five slices anterior and five slices posterior were identified (Fig. 1i). These two sections were, therefore, separated by approximately 18 mm in the rostral–caudal plane. All streamlines that passed through both regions of interest were retained as 'cingulum' pathways (Fig. 1i, see also Catani et al., 2002; Gong et al., 2005; Singh & Wong, 2010; Xie et al., 2005).

This procedure was repeated in each hemisphere for all 20 participants. As will be discussed later, a probabilistic overlay of the tract reconstructions from all 20 participants was made without the use of the further regions of interest. However, for the illustrations in Fig. 1, additional 'NOT' ROIs were used to exclude tracts that were inconsistent with known projections of the cingulum.

Download English Version:

https://daneshyari.com/en/article/10465012

Download Persian Version:

https://daneshyari.com/article/10465012

<u>Daneshyari.com</u>